Matrix Isolation and ab Initio Study of 1:1 Hydrogen-Bonded Complexes of H_2O_2 with Phosphorus and Sulfur Bases

James R. Goebel and Bruce S. Ault*

Department of Chemistry, University of Cincinnati, P.O. Box 210172, Cincinnati, Ohio 45221-0172

Janet E. Del Bene

Department of Chemistry, Youngstown State University, Youngstown, Ohio 44555, and Quantum Theory Project, University of Florida, Gainesville, Florida 32611

Received: August 23, 2001; In Final Form: October 15, 2001

Matrix isolation infrared spectroscopy has been combined with MP2/6-31+G(d,p) and MP2/aug′-cc-pVTZ calculations to characterize the 1:1 hydrogen-bonded complexes between H_2O_2 and bases containing phosphorus and sulfur as electron pair donor atoms. Most obvious from the spectra of the complexes HOOH:PH_3, HOOH:$P(CH_3)_3$, HOOH:SH_2, and HOOH:$S(CH_3)_2$ and their deuterated analogues is the shift to lower frequency of the hydrogen-bonded O−H or O−D stretching bands (ν_s) relative to isolated H_2O_2 and D_2O_2. The experimental shifts are in good agreement with the computed shifts. Shifted modes of both H_2O_2 and base subunits have been observed, along with the band for the intermolecular librational mode of each complex. Comparisons are made between the structures and spectral properties of these complexes and related complexes formed between H_2O_2 and corresponding N and O bases.

Introduction

Hydrogen peroxide is a molecule that is of interest in a large and diverse number of fields, including atmospheric chemistry and biochemistry.[1−3] Until recently, gas-phase, solvent-free studies of H_2O_2 were technically difficult. However, the development[4] and use of the hydrogen peroxide−urea complex (UHP) as a safe source of solvent-free gas-phase H_2O_2 has allowed initial studies[5−8] of the hydrogen-bonding capability of H_2O_2. This is an important development, since solution studies are complicated by the role of the solvent, to the extent that hydrogen peroxide has not been well characterized in hydrogen-bonded complexes. Early theoretical studies[9] characterized transition states and intermediates in the reaction chemistry of H_2O_2, but did not focus on hydrogen bonding. Mo et al.[10] have reported calculations on hydrogen-bonded complexes $(H_2O_2)_2$ and H_2O_2:H_2O.

The matrix isolation technique[11−13] was developed for the isolation, stabilization, and spectroscopic characterization of reactive intermediates, including hydrogen-bonded complexes. Recently, experimental studies were conducted in this laboratory to characterize hydrogen-bonded complexes of H_2O_2 with amines[5] and dimethyl ether.[6] Ab initio calculations were also carried out to provide energetic and structural information about these complexes. To further explore the ability of H_2O_2 to participate in hydrogen bonds, these joint experimental and theoretical studies have now been extended to the hydrogen-bonded complexes of H_2O_2 with phosphorus and sulfur bases. The structural, energetic, and spectral properties of these complexes will first be determined and discussed, and then compared to the corresponding complexes of H_2O_2 with nitrogen and oxygen bases.

* Corresponding author.

Experimental Section

All of the experiments in this study were carried out on conventional matrix isolation equipment,[14] with modification for the generation and deposition of H_2O_2, as described previously.[6] The temperature range for the vaporization of H_2O_2 in these experiments was 9−18 °C. PH_3 (Matheson) and H_2S:D_2S (Isotec) were introduced into the vacuum system from lecture bottles, and purified by repeated freeze−pump−thaw cycles at 77 K. $P(CH_3)_3$, $S(CH_3)_2$, and $S(CD_3)_2$ (all Aldrich) were placed in a glass finger attached to the sample manifold, and purified by repeated freeze−pump−thaw cycles at 77 K. Their room-temperature vapor pressure was employed to prepare the sample concentration of interest. Argon was used without further purification as the matrix gas in these experiments.

All of the experiments were conducted in the twin jet mode, in which samples of H_2O_2 and the base were each diluted in the matrix gas and deposited from separate deposition lines onto the 14 K cold window. In the early experiments, a traditional slow deposition rate of approximately 2 mmol/h from each manifold for 22−24 h was used. Later experiments were conducted using a fast deposition of approximately 15 mmol/h from each manifold for 3 h. Spectral features were essentially identical with slow and fast deposition. However, higher quality (less scattering) matrices were obtained with fast deposition. Spectra were then recorded on a Mattson Cygnus FTIR at 1 cm^{-1} resolution. The matrices were subsequently annealed to between 30 and 36 K and after re-cooling, additional spectra were recorded.

Method of Calculation

The structures of the complexes HOOH:SH_2, HOOH:$S(CH_3)_2$, HOOH:PH_3, and HOOH:$P(CH_3)_3$, and the corresponding monomers H_2O_2, SH_2, $S(CH_3)_2$, PH_3, and $P(CH_3)_3$ were optimized at second-order Møller−Plesset perturbation theory (MP2)[15−18]

10.1021/jp013262b CCC: $20.00
Published on Web 11/22/2001

with the 6-31+G(d,p) basis set.[19−22] Harmonic vibrational frequencies were computed to establish that the optimized structures are equilibrium structures on the potential surfaces, to evaluate zero-point vibrational energies, and to simulate vibrational spectra. Computed MP2/6-31+G(d,p) structures of hydrogen-bonded complexes are in reasonable agreement with experimental structures. Moreover, MP2/6-31+G(d,p) is the minimum level of theory that provides frequency shifts of the hydrogen-bonded X−H stretching band in agreement with experimental shifts, provided that anharmonicity corrections in the complexes are not unusually large.[23−25] The harmonic vibrational spectra of the deuterated analogues of monomers and complexes have also been computed.

For improved binding energies, single-point MP2/aug′-cc-pVTZ calculations were carried out on the optimized monomers and complexes. The valence triplet-split aug′-cc-pVTZ basis set is the aug-cc-pVTZ basis[26−28] with diffuse functions on all atoms except hydrogen. This basis set gives binding energies which approach basis-set converged binding energies, without correcting for basis-set superposition errors.[29] For all calculations on monomers and complexes, electrons below the valence shell were frozen in the Hartree−Fock molecular orbitals. These calculations were carried out using Gaussian 98[30] on the Cray SV1 computer at the Ohio Supercomputer Center.

Experimental Results

Before co-deposition experiments were run, blank spectra of trimethylphosphine (TMP), phosphine, dimethyl sulfide (DMS), and d6-dimethyl sulfide (d6-DMS)were obtained in separate experiments. The spectra agreed well with published data[31−35] and spectra previously obtained in this laboratory. Hydrogen sulfide experiments were performed using H_2S that was approximately 50% deuterated. Thus, all of these experiments contained a mixture of H_2S, HDS, and D_2S. The spectrum of this mixture agreed with published data[36] and spectra previously recorded in this laboratory.

H_2O_2 + TMP. In an initial experiment argon swept over UHP at 21 °C was co-deposited with a sample of Ar/TMP = 500/1. Several distinct product bands were noted, the most prominent of which was a medium intensity, relatively broad band at 3215 cm^{-1}. Four weak bands were observed at 1298, 721, 717, and 606 cm^{-1}; selected spectral regions are shown in Figure 1. Upon annealing this matrix to 36 K, all of the product bands grew in roughly the same proportions.

A total of 10 experiments were conducted in which the temperature of the UHP (concentration of H_2O_2) was varied from 9 °C to 21 °C and the Ar/TMP concentration was varied from 250/1 to 1000/1. In all experiments the bands at 3215, 721, 717, and 606 cm^{-1} were present with intensities proportional to reactant concentrations. In all but the lowest concentration experiment, the very weak band at 1298 cm^{-1} was also observed. All matrices were annealed, and all bands grew at the same rate.

D_2O_2 + TMP. Two experiments were conducted with d2-UHP in which the temperature was 15 °C in one experiment and 18 °C in the other, with an Ar/TMP concentration of 500/1 in both. A product band with an intensity that depended on the concentration of D_2O_2 was seen at 2392 cm^{-1}, as shown in Figure 2. In both experiments the intensity of this band grew upon annealing the matrix, and no new product bands were formed.

H_2O_2 and PH_3. In an initial experiment argon swept over UHP at 15 °C was co-deposited with a sample of Ar/PH_3 = 500/1. Several distinct product bands were noted, the most prominent of which was an intense, relatively broad band at 3444 cm^{-1}. In addition, three bands occurred at 2364, 1292, and 465 cm^{-1}. Upon annealing this matrix to 36 K all of the product bands grew in roughly the same proportions, and one new band appeared at 3451 cm^{-1}.

A total of eight experiments were conducted in which the temperature of UHP (concentration of H_2O_2) varied from 9 °C to 18 °C and the Ar/PH_3 concentration varied from 250/1 to

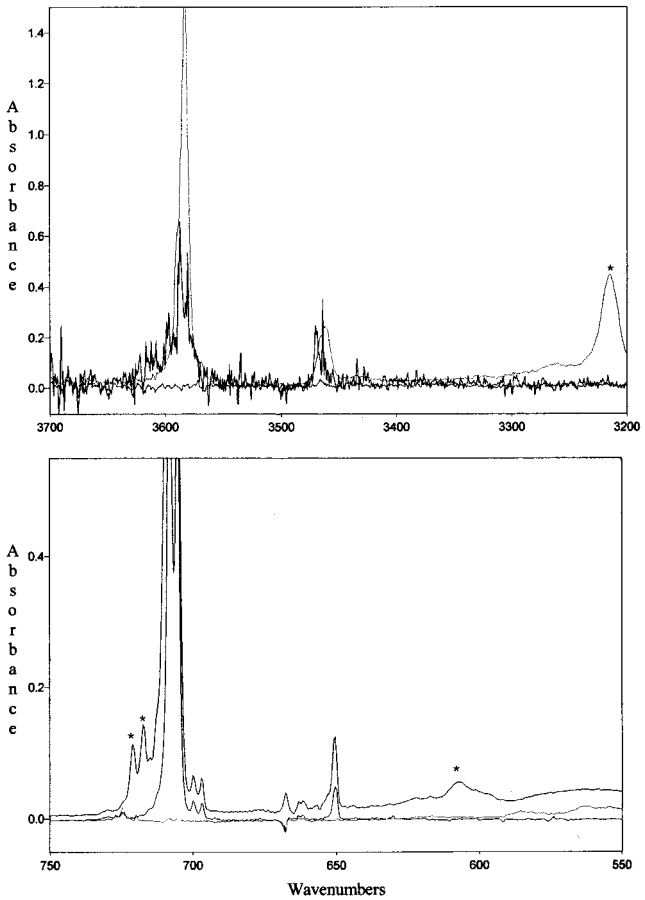

Figure 1. Infrared spectrum of a matrix prepared by passing argon over the solid H_2O_2:urea complex, and co-depositing with a sample of Ar/$P(CH_3)_3$ = 500/1 overlaid on a blank spectrum of Ar/$P(CH_3)_3$ = 500 and the spectrum of a matrix of Ar + H_2O_2. Bands marked with an * are due to the 1:1 hydrogen-bonded complex.

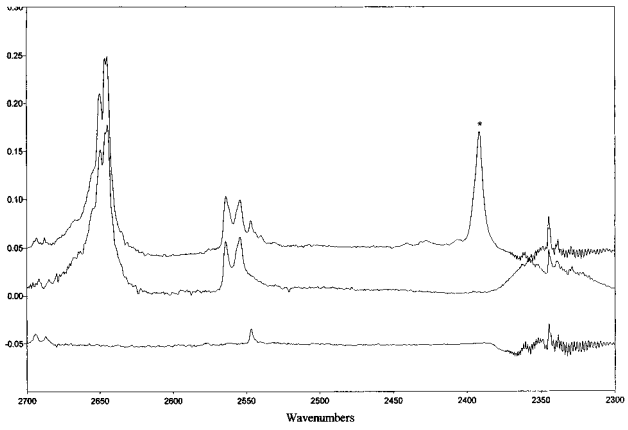

Figure 2. Infrared spectrum of a matrix prepared by passing argon over the solid D_2O_2:urea complex, and co-depositing with a sample of Ar/$P(CH_3)_3$ = 500/1 (top trace) compared to a blank spectrum of Ar/$P(CH_3)_3$ = 500/1 (middle trace) and a matrix of Ar + D_2O_2 (bottom trace). The band marked with an * is due to the 1:1 hydrogen-bonded complex.

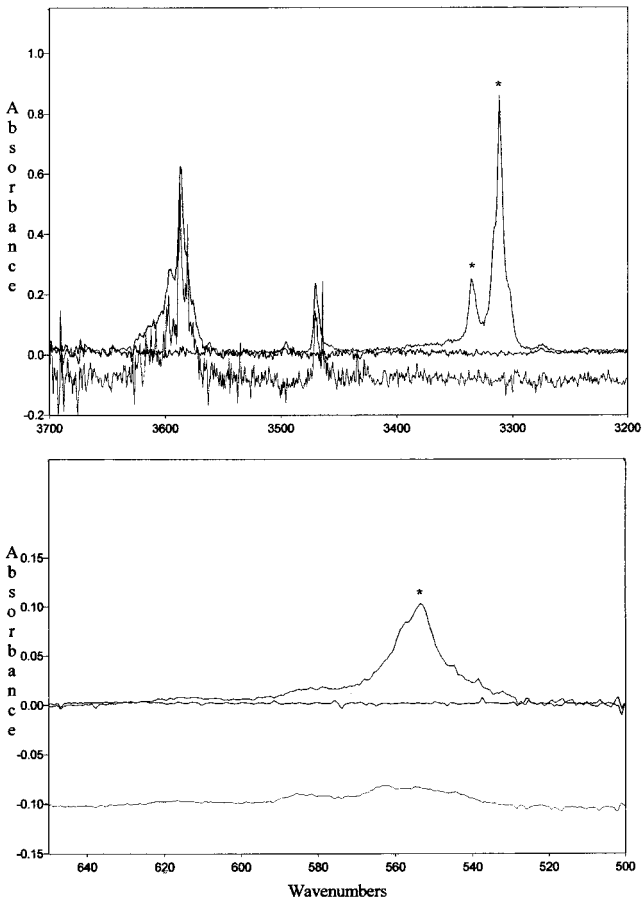

Figure 3. Infrared spectrum of a matrix prepared by passing argon over the solid H_2O_2:urea complex, and co-depositing with a sample of $Ar/S(CH_3)_2 = 500/1$ (top trace) compared to a blank spectrum of $Ar/S(CH_3)_2 = 500/1$ (middle trace) and the spectrum of a matrix of Ar + H_2O_2 (bottom trace). Bands marked with an * are due to the 1:1 hydrogen-bonded complex.

1000/1. In all experiments, bands at 3444, 2364, 1292, and 465 cm^{-1} were present. The intensities of these bands depended directly on the reactant concentrations. When the matrices were annealed, all bands grew at the same rate. Two new bands appeared at 3451 and 987 cm^{-1}, with intensities proportional to the concentration of the reactants.

D_2O_2 + PH_3. One experiment was performed using D_2O_2 and PH_3. In addition to the bands due to reactants, several new product bands were observed. These occurred at 2550, 2364, 986, and 964 cm^{-1}, with the band at 2550 cm^{-1} being the most intense. Upon annealing, all product bands increased in intensity, and no new product bands appeared.

H_2O_2 + DMS. In an initial experiment argon swept over UHP at 18 °C was co-deposited with a sample of Ar/DMS = 250/1. Several distinct product bands were noted, the most prominent of which was an intense, relatively broad band at 3312 cm^{-1}. In addition, four bands were observed at 3336, 1286, 981, and 554 cm^{-1}; selected spectral regions are shown in Figure 3. Upon annealing this matrix to 36 K, all of the product bands grew in roughly the same proportion except for the band at 3336 cm^{-1}, which disappeared.

A total of eight experiments were conducted in which the temperature of the UHP (concentration of H_2O_2) changed from 9 °C to 21 °C and the Ar/DMS concentration changed from 250/1 to 1000/1. In all experiments bands at 3312, 3336, 1286, and 554 cm^{-1} were present. The intensities of these bands varied according to the concentration of the reactants. The band at 981 cm^{-1} observed in the first experiment was not present in any other experiment, and was probably due to a contaminant. All matrices were annealed, with results similar to the first experiment.

H_2O_2 + d6-DMS. Two experiments were performed with peroxide and perdeuterated DMS. In an initial experiment argon swept over UHP at 15 °C was co-deposited with a sample of Ar/d6-DMS = 500/1. Several distinct product bands were noted, the most prominent of which was an intense, broad band at 3311 cm^{-1}. Three other bands occurred at 3335, 1286, and 553 cm^{-1}. When the matrix was annealed to 36 K all product bands except for the 3335 cm^{-1} band grew in roughly the same proportions. The band at 3335 cm^{-1} disappeared after annealing, and a new band appeared at 751 cm^{-1}. In the second experiment UHP at 9 °C was co-deposited with Ar/d6-DMS = 500/1. The same product bands were observed, but they had proportionally lower intensities compared to the first experiment. After annealing, similar results were obtained, although the band at 751 cm^{-1} did have the same i:ntensity in both experiments.

D_2O_2 + DMS. One experiment was run using D_2O_2 and DMS. In addition to the bands from each reactant, two new bands were observed. The more intense band occurred at 2458 cm^{-1}, and the less intense band was found at 2475 cm^{-1}. Upon annealing, the intensity of the band at 2458 cm^{-1} increased and the band at 2475 cm^{-1} disappeared.

H_2O_2 + $H_2S;D_2S$. In an initial experiment argon swept over UHP at 15 °C was co-deposited with a sample of $Ar/(H_2S;D_2S)$ = 250/1. Several distinct product bands were noted, including an intense, broad band at 3456 cm^{-1} and two weaker bands at 1296 and 1290 cm^{-1}. Upon annealing this matrix all of the product bands grew in roughly the same proportions.

A total of four other experiments were conducted in which the temperature of the UHP (concentration of H_2O_2) was varied from 12 °C to 18 °C and the $Ar/(H_2S;D_2S)$ concentration varied from 250/1 to 1000/1. In these experiments bands at 3456, 1296, and 1290 c:m^{-1} were present with intensities that depended directly on reaction concentrations. In the experiment run at the highest concentration (Ar/UHP at 18 °C: $Ar/(H_2S;D_2S)$ = 250/1) a very weak, broad band at 466 cm^{-1} was also observed. Upon annealing, the product bands grew smoothly in proportion to concentration, except for the band at 466 cm^{-1} which grew to a lesser extent.

D_2O_2 and $H_2S;D_2S$. A single experiment was conducted in which argon swept over d2-UHP at 18 °C was co-deposited with a sample of $Ar/(H_2S;D_2S)$ = 250/1. Two distinct product bands were noted, a broad band of medium intensity at 2556 cm^{-1}, and a weaker band at 1016 cm^{-1}.

Results of ab Initio Calculations

The equilibrium structures of the complexes $HOOH:PH_3$, $HOOH:P(CH_3)_3$, $HOOH:SH_2$, and $HOOH:S(CH_3)_2$, have C_1 symmetry. The MP2/6-31+G(d,p) intermolecular O−P and O−S distances, the hydrogen-bonded O−H distances, and the H−O−P and H−O−S angles which measure the extent to which the hydrogen bonds deviate from linearity are presented for the equilibrium structures in Table 1. Table 1 also reports the MP2/aug′-cc-pVTZ electronic binding energies and binding enthalpies for selected isotopomers.

The complex $HOOH:PH_3$ is the most weakly bound complex, with an electronic binding energy of −3.9 kcal/mol, and a binding enthalpy of only −2.6 kcal/mol. This complex has the longest intermolecular distance of 3.412 Å. The hydrogen-bonded O−H distance is 0.977 Å, which is only 0.007 Å longer

TABLE 1: Equilibrium Distances (Å) and Angles (°), and Binding Energies and Enthalpies (kcal/mol) for Complexes of H_2O_2 with PH_3, $P(CH_3)_3$, SH_2, and $S(CH_3)_2$ and Selected Deuterated Analogues

complex	R_e(O−X)[a]	R_e(O−H)[b]	<H−O−X[a,c]	Δ_e	Δ^0
HOOH:PH_3	3.412	0.977	11	−3.9	−2.6
DOOD:PH_3					−2.7
HOOH:$P(CH_3)_3$	3.257	0.984	18	−7.3	−6.1
DOOD:$P(CH_3)_3$					−6.2
HOOH:SH_2	3.324	0.976	21	−4.4	−2.8
HOOH:SD_2					−3.1
DOOD:SH_2					−2.9
DOOD:SD_2					−3.1
HOOH:$S(CH_3)_2$	3.262	0.981	16	−7.5	−6.3
HOOH:$S(CD_3)_2$					−6.4
DOOD:$S(CH_3)_2$					−6.4

[a] For complexes with SH_2 and $S(CH_3)_2$, X = S; for complexes with PH_3 and $P(CH_3)_3$, X = P. [b] The O−H bond length in H_2O_2 is 0.970 Å. [c] <H−O−X = 0° corresponds to a linear O−H...X hydrogen bond.

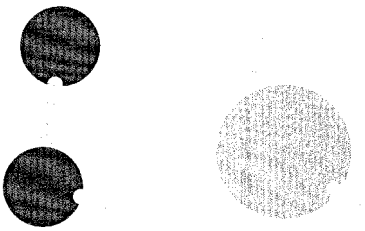

Figure 4. Structure of the HOOH:SH_2 complex, computed at the MP2/6-31+G(d,p) level of theory.

than the O−H distance in H_2O_2. The hydrogen bond in this complex is closest to linear, with an H−O−P angle of 11°.

The complex HOOH:SH_2 has an electronic binding energy of −4.4 kcal/mol, which is 0.5 kcal/mol greater than HOOH:PH_3. However, the zero-point vibrational energy correction in this complex leads to a binding enthalpy of −2.8 kcal/mol, only 0.2 kcal/mol greater than the binding enthalpy of HOOH:PH_3. Similarly, DOOD:SH_2 is 0.2 kcal/mol more stable than DOOD:PH_3. The intermolecular O−S distance is 3.324 Å, almost 0.1 Å shorter than the O−P distance in HOOH:PH_3. The hydrogen-bonded O−H distance in HOOH:SH_2 is 0.976 Å, similar to the O−H distance in HOOH:PH_3. The hydrogen bond deviates from linearity by 21° in HOOH:SH_2. Figure 4 illustrates the equilibrium structure of HOOH:SH_2.

Substitution of CH_3 groups for H leads to complexes HOOH:$S(CH_3)_2$ and HOOH:$P(CH_3)_3$ which have significantly increased binding energies, shorter intermolecular distances, and longer hydrogen-bonded O−H distances than HOOH:PH_3 and HOOH:SH_2. HOOH:$P(CH_3)_3$ and HOOH:$S(CH_3)_2$ have binding energies of −7.3 and −7.5 kcal/mol, respectively. Corresponding isotopomers with phosphorus as the base are 0.2 kcal/mol less stable than those with sulfur as the base. The intermolecular O−P and O−S distances in HOOH:$P(CH_3)_3$ and HOOH:$S(CH_3)_2$ are similar at 3.257 and 3.262 Å, as are the hydrogen-bonded O−H distances of 0.984 and 0.981 Å, respectively. The hydrogen bond deviates from linearity by 16° and 18° in these two complexes, respectively.

Discussion

Product Identification. Twin-jet co-deposition of samples of Ar/H_2O_2 with each of the third-row bases employed in this study led to new product bands throughout the spectrum. Band positions for all pairs of reactants are given in Tables 2 and 3. The product bands are typified by the bands in the H_2O_2:TMP system at 3215, 1298, 721, 717, and 606 cm^{-1}. These bands

TABLE 2: Band Positions and Assignments for the 1:1 Complexes of H_2O_2 with $P(CH_3)_3$ and PH_3

complex	ν(expt)	$\Delta\nu$(expt)	$\Delta\nu$(calc)	assignment
H_2O_2:PH_3	3444 cm^{-1}	−146	−137	ν_s, O−H stretch
	2364	+19	+36	PH_3 antisym. stretch
	1292	+22	+25	ν_b, O−O−H bend
	465		567[a]	ν_l, libration
D_2O_2:PH_3	2550	−94	−97	ν_s, O−D stretch
	2364	+19	+36	PH_3 antisym. stretch
	964	+13	+18	ν_b, O−O-D bend
H_2O_2:$P(CH_3)_3$	3215 cm^{-1}	−375	−285	ν_s, O−H stretch
	1298	+28	+26	ν_b, O−O−H bend
	717, 721	+13	+11	PC_3 antisym. stretch
	606		632[a]	ν_l, libration
D_2O_2:$P(CH_3)_3$	2392	−252	−204	ν_s, O−D stretch

[a] The absolute value of the frequency.

TABLE 3: Band Positions and Assignments for the 1:1 Complexes of H_2O_2 with $S(CH_3)_2$ and H_2S

complex	ν(expt)	$\Delta\nu$(expt)	$\Delta\nu$(calc)	assignment
H_2O_2:$S(CH_3)_2$	3312 cm^{-1}	−278	−224	ν_s, O−H stretch
	1286	+16	+15	ν_b, O−O−H bend
	554		575[a]	ν_l, libration
D_2O_2:$S(CH_3)_2$	2458	−186	−159	ν_s, O−D stretch
H_2O_2:$S(CD_3)_2$	3311	−279	−224	ν_s, O−H stretch
	1286	+16	+15	ν_b, O−O−H bend
	553		575[a]	ν_l, libration
H_2O_2:H_2S/D_2S	3456	−134	−117	ν_s, O−H stretch
	1291	+21	+20	ν_b, O−O−H bend
	466		536[a]	ν_l, libration
D_2O_2:H_2S/D_2S	2556	−88	−83	ν_s, O−D stretch

[a] The absolute value of the frequency.

are typical in that one band occurs in the low 3000 cm^{-1} region of the spectrum, one or more bands are found near H_2O_2 or base absorptions, and one new low-energy band (the band at 606 cm^{-1} in H_2O_2:TMP) appears that is not near a H_2O_2 or base absorption. Such bands were observed in all experiments with a given pair of reactants, regardless of reactant concentration, except that the lowest energy band was not observed in the more dilute experiments. Moreover, the intensities of these bands did not change abruptly upon annealing, but increased smoothly in approximately the same intensity ratios. These observations suggest that a single product was formed upon initial deposition.

With the exception of the band in the 3000 cm^{-1} region and the lowest energy band, all other bands lie near bands observed for either H_2O_2 or the base. This suggests that a weakly bound complex is formed in which the two monomers are perturbed but maintain their structural integrity. This observation is consistent with the results of previous investigations[37] of hydrogen-bonded complexes containing TMP with other proton donors.

The highest energy band in each system (at 3215 cm^{-1} in the H_2O_2:TMP system) is not near any reactant band, but is several hundred wavenumbers to the red of the O−H stretches in H_2O_2. A strongly red-shifted O−H stretch of H_2O_2 is consistent with, and supports formation of a hydrogen-bonded complex between H_2O_2 and each base,[38] with H_2O_2 serving as the proton donor. This is also consistent with earlier studies[5,6] of hydrogen-bonded complexes of H_2O_2 with second-row bases, and with studies[37,39] in which third-row bases were involved in hydrogen bond formation.

The experimental data strongly suggest that the single product formed in each experiment is a 1:1 hydrogen-bonded complex of H_2O_2 with a sulfur or phosphorus base. The fact that the product bands are observed at quite low concentrations argues

TABLE 4: Selected Equilibrium Distances (R_e, Å) and Angles (<,°), Binding Energies (ΔE, kcal/mol), and Frequency Shifts of the O−H Stretching Band ($\Delta\nu$, cm^{-1}) for Corresponding Complexes of H_2O_2 with N, O, P, and S Bases

complex	R_e(O−X, O−H)[a]	<H−O−X[a,b]	ΔE_e	($\Delta\nu_s$, calc)	($\Delta\nu_s$, expt)
HOOH:NH_3[c]	2.810, 0.990	8	−9.0	−400	−385
HOOH:PH_3	3.412, 0.977	11	−3.9	−137	−146
HOOH:$N(CH_3)_3$[c]	2.727, 1.004	0	−11.3	−683	−781
HOOH:$P(CH_3)_3$	3.257, 0.984	18	−7.3	-285	−375
HOOH:OH_2	2.789, 0.979	21	−7.2	−158	−130
HOOH:SH_2	3.324, 0.976	21	−4.4	−117	−134
HOOH:$O(CH_3)_2$[d]	2.737, 0.985	8	−8.4	−239	−234
HOOH:$S(CH_3)_2$	3.262, 0.981	16	−7.5	−224	−278

[a] X is the hydrogen-bonded N, P, O, or S atom of the base. [b] <H−O−X = 0° corresponds to a linear hydrogen bond. A positive value of this angle indicates that the hydrogen-bonded proton lies on the opposite side of the intermolecular O−X line relative to the second oxygen of HOOH:$N(CH_3)_3$. See Figure 4. [c] Data taken from ref 5. [d] Data taken from ref 6.

against the single product being a higher complex with 2:1 or 1:2 H_2O_2:base stoichiometry. Further, it would be difficult to envision formation of a higher complex without initial formation of the 1:1 complex, yet only a single product was observed in all experiments. This conclusion is also strongly supported by the MP2/6-31+G(d,p) calculations, which demonstrate that the corresponding 1:1 H_2O_2:base hydrogen-bonded complexes are stable. Further, the computed MP2/6-31+G(d,p) spectral data are in very good agreement with the experimental, as will be shown below. *Therefore, both experiment and theory support the formation of 1:1 H_2O_2:base hydrogen-bonded complexes in the experiments performed in this study.*

It should be noted that a previous matrix study of H_2O co-deposited with H_2S reported[40] the formation of two different 1:1 hydrogen-bonded complexes, one with H_2O as the proton donor, the other with H_2S as the donor. However, no evidence of the existence of a second H_2O_2:H_2S complex was found in the present study. Such a complex should have a clearly shifted and intensified S−H stretching band, but such a band was not observed. Moreover, a search of the MP2/6-31+G(d,p) H_2O_2:H_2S potential energy surface did not find a second equilibrium structure.

Band Assignments

As noted above, the spectrum of each reactant pair exhibits an intense, relatively broad absorption band several hundred wavenumbers to the red of the O−H stretches of H_2O_2. The exact position of this band varied with the base, from 3456 cm^{-1} with H_2S to 3215 cm^{-1} with TMP. This band also shifted significantly to lower energy when D_2O_2 was substituted for H_2O_2, as evident from Tables 2 and 3. The ν_H/ν_D shift ratios range from 1.34 to 1.35 in the different complexes. Thus, the anharmonicity of the O−H stretching mode in the complexes arises primarily in the H_2O_2 monomer, where ν_H/ν_D is 1.36. This band did not shift when the base subunit was deuterated (D_2S and d_6-DMS), again indicating that it is associated with a vibrational mode of H_2O_2. These spectral characteristics are exactly those of a hydrogen-bonded X−H stretch in an X−H−Y hydrogen bond. Thus, these shifted bands are assigned to the O−H (or O−D) stretch in the 1:1 hydrogen-bonded complexes. It should be noted that since the H_2S experiments contained a mixture of H_2S, HDS, and D_2S, the band at 3456 cm^{-1} is a superposition of O−H stretching bands in HOOH:SH_2, HOOH:SD_2, and HOOH:SHD. Previous studies[5,6] and the d_6-DMS data, above, have shown that deuteration of the proton acceptor has little effect on the O−H stretching band. Moreover, as can be seen from Tables 2 and 3, the computed MP2/6-31+G(d,p) band shifts for the O−H and O−D stretches are in quite good agreement with the experimental shifts, again supporting this assignment.

In each experiment involving H_2O_2, a band was observed between 1290 and 1300 cm^{-1}. This band is unambiguously assigned to the H_2O_2 moiety, since it shifted upon D_2O_2 substitution, but did not shift upon deuteration of the base. A second spectral signature of hydrogen bonding is a blue shift of the band corresponding to a bending mode of the proton-donor species.[37] For H_2O_2, this band is observed at 1270 cm^{-1}. Blue shifts of 22, 28, and 16 cm^{-1} were found in the complexes of H_2O_2 with PH_3, $P(CH_3)_3$, and SH_2, respectively. These shifts are consistent with shifts observed[4−7] for other hydrogen-bonded complexes containing H_2O_2, and are in excellent agreement with the calculated MP2/6-31+G(d,p) blue shifts of 25, 26, and 15 cm^{-1}, respectively.

Except for the H_2O_2:H_2S system for which the product yield was very low, additional absorptions were observed in each spectrum near bands associated with the base. These are typified by the two bands at 721 and 717 cm^{-1} for H_2O_2:TMP, and the band at 2364 cm^{-1} for H_2O_2:PH_3. In a hydrogen-bonded complex, the base subunit is weakly perturbed, and slightly shifted base vibrational bands are often observed. Their proximity to the parent bands makes assignments straightforward. The computed shifts of these bands and their assignments are reported in Tables 2 and 3.

The lowest energy product band for each system remains to be assigned. This band was observed for the H_2O_2 complexes with PH_3, TMP, H_2S, and DMS at 465, 606, 466, and 554 cm^{-1}, respectively. Neither H_2O_2 nor any base has vibrational modes near these bands, so assignment to a perturbed mode of either monomer is *not* appropriate. However, the formation of a 1:1 complex between two nonlinear molecules results in the loss of 3 translational and 3 rotational degrees of freedom, and the creation of 6 new intermolecular vibrational modes which typically lie at very low frequencies. One of these modes, the libration mode, has been observed in the spectral region between 500 and 1000 cm^{-1} in a number of hydrogen-bonded complexes.[5,38,39,41,42] In general, the more strongly bound the complex, the higher the frequency of the librational mode. The computed MP2/6-31+G(d,p) frequencies for the libration mode are also reported in Tables 2 and 3, and are in excellent agreement with the experimental frequencies. Thus, these low-frequency bands are assigned to the librational mode in each complex.

Comparisons with Complexes of H_2O_2 with O and N Bases

Table 4 presents equilibrium intermolecular O−X (X = N, P, O, S) and hydrogen-bonded O−H distances, the angle between the O−H bond and the hydrogen-bonding O−X axis, MP2/aug′-cc-pVTZ binding energies, and computed and experimental frequency shifts of the proton-stretching band in

complexes HOH:NH_3, HOOH:PH_3, HOOH:$N(CH_3)_3$, HOOH:$P(CH_3)_3$, HOH:OH_2, HOOH:SH_2, HOOH:$O(CH_3)_2$, and HOOH:$S(CH_3)_2$. From these data it is apparent that complexes of H_2O_2 with second-row ($n = 2$) bases are more stable that the corresponding complexes with third-row ($n = 3$) bases. Thus, HOOH:NH_3 is 5.1 kcal/mol more stable than HOOH:PH_3, and HOOH:OH_2 is 2.8 kcal/mol more stable than HOOH:SH_2. Methyl substitution preferentially stabilizes complexes with third-row bases, with the result that the energy difference between corresponding complexes decreases. HOOH:$N(CH_3)_3$ is still 4.0 kcal/mol more stable than HOOH:$P(CH_3)_3$, but HOOH:$O(CH_3)_2$ is only 0.9 kcal/mol more stable than HOOH:$S(CH_3)_2$.

Although frequency shifts may correlate with binding energies in a closely related series of complexes, such a correlation is generally not observed. Frequency shifts are dependent on the structures of hydrogen-bonded complexes, including the X−H distances in an X−H−Y hydrogen bond, the extent to which the hydrogen bond deviates from linearity, and variations in hydrogen bond type. Moreover, frequency shifts are determined by the nature of the intermolecular potential surface, which may introduce larger anharmonicity corrections in either the ground or first-excited state of the X−H stretching mode relative to the monomer, and on the nature of the medium in which the experimental measurements are made.[43−48] Nevertheless, among the eight complexes with H_2O_2 as the proton donor, the largest computed and experimental shifts of the hydrogen-bonded O−H stretching band are found for HOOH:$N(CH_3)_3$. The computed frequency shift for this complex is 300 cm^{-1} greater than the computed shift for any other complex, while the experimental shift is 400 cm^{-1} greater. This complex has the largest binding energy, the longest hydrogen-bonded O−H distance, and a hydrogen bond which is linear. In general, as the hydrogen-bonded O−H distance increases, the frequency of the O−H stretching band tends to decrease.

Finally, it should be noted that the most commonly used measure of basicity, namely gas-phase proton affinities, do not correlate with binding energies or frequency shifts. For example, the proton affinities of $N(CH_3)_3$ and $P(CH_3)_3$ are very similar at 225 and 227 kcal/mol, respectively.[49] Yet, the binding energies of the complexes HOOH:$N(CH_3)_3$ and HOOH:$P(CH_3)_3$ are quite different at −11.3 and −7.3 kcal/mol, respectively, and the computed and experimental shifts of the O−H stretching band are 400 cm^{-1} greater for HOOH:$N(CH_3)_3$.

Acknowledgment. The National Science Foundation is gratefully acknowledged for support of this research through Grant CHE 9877076.

References and Notes

(1) Gregoire, P. J.; Chaumerliac, N.; Nickerson, E. C. *J. Atmos. Chem.* **1994**, *18*, 247.

(2) Sakugawa, H.; Kaplan, I. R. In *Gaseous Pollutants*; Nriagu, J. O., Ed.; John Wiley and Sons: New York, 1992; Vol. 24.

(3) .*Oxidative Stress, Cell Activation and Viral Infection*; Pasquier, C., Ed.; Birkhauser Verlag: Basel, Boston, 1994; p 358.

(4) Petterson, M.; Tuominen, S.; Rasanen, M. *J. Phys. Chem.* **1997**, *101*, 1166.

(5) Goebel, J. R.; Ault, B. S.; Del Bene, J. E. *J. Phys. Chem. A* **2001**, *105*, 6430.

(6) Goebel, J.; Ault, B. S.; Del Bene, J. E. *J. Phys. Chem. A* **2000**, *104*, 2033.

(7) Lundell, J.; Jolkkonen, S.; Khriachtchev, L.; Pettersson, M.; Rasanen, M. *Chem.—Eur. J.* **2001**, *7*, 1670.

(8) Engdahl, A.; Nelander, B. *Phys. Chem. Chem. Phys.* **2000**, *2*, 3967.

(9) Bach, R. D.; Su, M.-D.; Schlegel, H. B. *J. Am. Chem. Soc.* **1994**, *116*, 5379. Bach, R. D.; Owensby, A. L.; Gonzalez, C.; Schlegel, H. B.; McDouall, J. J. W. *J. Am. Chem. Soc.* **1991**, *113*, 6001.

(10) Mo, O.; Yanez, M.; Rozas, I.; Elguero, J. *J. Chem. Phys.* **1994**, *100*, 2871.; Mo, O.; Yanez, M.; Rozas, I.; Elguero, J. *Chem. Phys. Lett.* **1994**, *219*, 45.

(11) Cradock, S.; Hinchcliffe, A. *Matrix Isolation*; Cambridge University Press: Cambridge, 1975.

(12) Whittle, E.; Dows, D. A.; Pimentel, G. C. *J. Chem. Phys.* **1954**, *22*, 1943.

(13) *Chemistry and Physics of Matrix Isolated Species*; Andrews, L., Moskovitz, M., Eds.; Elsevier Science Publishers: Amsterdam, 1989.

(14) Ault, B. S. *J. Am. Chem. Soc.* **1978**, *100*, 2426.

(15) Bartlett, R. J.; Silver, D. M. *J. Chem. Phys.* **1975**, *62*, 3258.

(16) Bartlett, R. J.; Purvis, G. D. *Int. J. Quantum Chem.* **1978**, *14*, 561.

(17) Pople, J. A.; Binkley, J. S.; Seeger, R. *Int. J. Quantum Chem. Quantum Chem. Symp.* **1976**, *10*, 1.

(18) Krishnan, R.; Pople, J. A. *Int. J. Quantum Chem.* **1978**, *14*, 91.

(19) Hehre, W. J.; Ditchfield, R.; Pople, J. A. *J. Chem. Phys.* **1972**, *56*, 2257.

(20) Hariharan, P. C.; Pople, J. A. *Theor. Chim. Acta* **1973**, *28*, 213.

(21) Spitznagel, G. W.; Clark, T.; Chandrasekhar, J.; Schleyer, P. v. R. *J. Comput. Chem.* **1982**, *3*, 363.

(22) Clark, T.; Chandrasekhar, J.; Spitznagel, G. W.; Schleyer, P. v. R. *J. Comput. Chem.* **1983**, *4*, 294.

(23) Del Bene, J. E.; Person, W. B.; Szczepaniak, K. *J. Phys Chem.* **1995**, *99*, 10705.

(24) Del Bene, J. E.; Shavitt, I. In *Molecular Interactions: From van der Waals to Strongly Bound Complexes*; Scheiner, S., Ed.; John Wiley and Sons: Chichester, U.K., 1997; pp 157−179.

(25) Del Bene, J. E. Hydrogen Bonding. In *The Encyclopedia of Computational Chemistry*; Schleyer, P. v. R., Allinger, N. L., Clark, T., Gasteiger, J., Kollman, P. A., Schaefer, H. F. III., Scheiner, P. R., Eds.; John Wiley and Sons: Chichester, U.K., 1998; Vol. 2, pp 1263−1271.

(26) Dunning, T. H., Jr. *J. Chem. Phys.* **1989**, *90*, 1007.

(27) Kendall, R. A.; Dunning, T. H., Jr.; Harrison, R. J. *J. Chem. Phys.* **1992**, *96*, 1358.

(28) Woon, D. E.; Dunning, T. H., Jr. *J. Chem. Phys.* **1993**, *98*, 1358.

(29) Dunning, T. H., Jr. *J. Phys. Chem. A* **2000**, *104*, 9062.

(30) Frisch, M. J.; Trucks, G. W.; Schlegel, H. B.; Scuseria, G. E.; Robb, M. A.; Cheeseman, J. R.; Zakrzewski, V. G.; Montgomery, J. A., Jr.; Stratmann, R. E.; Burant, J. C.; Dapprich, S.; Millam, J. M.; Daniels, A. D.; Kudin, K. N.; Strain, M. C.; Farkas, O.; Tomasi, J.; Barone, V.; Cossi, M.; Cammi, R.; Mennucci, B.; Pomelli, C.; Adamo, C.; Clifford, S.; Ochterski, J.; Petersson, G. A.; Ayala, P. Y.; Cui, Q.; Morokuma, K.; Malick, D. K.; Rabuck, A. D.; Raghavachari, K.; Foresman, J. B.; Cioslowski, J.; Ortiz, J. V.; Baboul, A. G.; Stefanov, B. B.; Liu, G.; Liashenko, A.; Piskorz, P.; Komaromi, I.; Gomperts, R.; Martin, R. L.; Fox, D. J.; Keith, T.; Al-Laham, M. A.; Peng, C. Y.; Nanayakkara, A.; Gonzalez, M.; Challacombe, M.; Gill, P. M. W.; Johnson, B.; Chen, W.; Wong, M. W.; Andres, J. L.; Gonzalez, C.; Head-Gordon, M.; Replogle, E. S.; Pople, J. A. *Gaussian 98*; Gaussian, Inc.: Pittsburgh, PA, 1998.

(31) Bouquet, G.; Bigorne, M. *Spectrochim. Acta* **1967**, *23A*, 1169.

(32) Wagstaff, F. J.; Thompson, K. W. *Trans. Faraday. Soc.* **1962**, *18*, 977.

(33) McConaghie, V. M.; Nielsen, H. H. *J. Chem. Phys.* **1953**, *21*, 1836.

(34) Allkins, J. R.; Hendra, P. J. *Spectrochim. Acta* **1966**, *22*, 2075.

(35) Geiseler, G.; Hanschmann, G. *J. Mol. Struct.* **1972**, *11*, 283.

(36) Barnes, A. J.; Howells, J. D. R. *J. Chem. Soc., Faraday Trans. 2* **1972**, *68*, 737.

(37) (a) Andrews, L. *J. Phys. Chem.* **1984**, *88*, 2940. (b) Arlinghaus, R. T.; Andrews, L. *J. Chem. Phys.* **1984**, *81*, 4341.

(38) Pimentel, G. C.; McClellan, A. L. *The Hydrogen Bond*; W. H. Freeman: San Francisco, 1960.

(39) Arlinghaus, R. T.; Andrews, L. *Inorg. Chem.* **1985**, *24*, 1523.

(40) Barnes, A. J.; Bentwood, R. M.; Wright, M. P. *J. Mol. Struct.* **1984**, *118*, 97.

(41) Johnson, G. L.; Andrews, L. *J. Am. Chem. Soc.* **1982**, *104*, 3043.

(42) Andrews, L.; Johnson, G. L. *J. Chem. Phys.* **1983**, *79*, 3670.

(43) Del Bene, J. E.; Mettee, H. D. *J. Phys. Chem.* **1993**, *97*, 9650.

(44) Hunt, R. D.; Andrews, L. *J. Phys. Chem.* **1992**, *96*, 6945.

(45) Del Bene, J. E.; Person, W. B.; Szczepaniak, K. *Mol. Phys.* **1996**, *89*, 47.

(46) Del Bene, J. E.; Jordan, M. J. T. *Int. Rev. Phys. Chem.* **1999**, *18*, 119.

(47) Jordan, M. J. T.; Del Bene, J. E. *J. Am. Chem. Soc.* **2000**, *122*, 2101.

(48) Andrews, L.; Wang, X.; Mielke, Z. *J. Phys. Chem. A* **2001**, *105*, 6054.

(49) Lias, S. G.; Liebman, J. F.; Levin, R. D. *J. Phys. Chem. Ref. Data* **1984**, *13*, 695.